Exponential distribution of long heart beat intervals during atrial fibrillation and their relevance for white noise behaviour in power spectrum

Thomas Hennig (`thomas.hennig@tu-ilmenau.de`) and Philipp Maass (`philipp.maass@tu-ilmenau.de`)
Institut für Physik, Technische Universität Ilmenau, 98684 Ilmenau, Germany

Junichiro Hayano (`hayano@med.nagoya-cu.ac.jp`)
Third Department of Internal Medicine, Nagoya City University Medical School, Nagoya 467, Japan

Stefan Heinrichs (`stefan.heinrichs@uni-konstanz.de`)
Fachbereich Physik, Universität Konstanz, 78457 Konstanz, Germany

10 March 2006

Abstract. The statistical properties of heart beat intervals of 130 long-term surface electrocardiogram recordings during atrial fibrillation (AF) are investigated. We find that the distribution of interbeat intervals exhibits a characteristic exponential tail, which is absent during sinus rhythm, as tested in a corresponding control study with 72 healthy persons. The rate γ of the exponential decay lies in the range 3-12 Hz and shows diurnal variations. It equals, up to statistical uncertainties, the level of the previously uncovered white noise part in the power spectrum, which is also characteristic for AF. The overall statistical features can be described by decomposing the intervals into two statistically independent times, where the first one is associated with a correlated process with $1/f$ noise characteristics, while the second one belongs to an uncorrelated process and is responsible for the exponential tail. It is suggested to use γ as a further parameter for a better classification of AF and for the medical diagnosis. The relevance of the findings with respect to a general understanding of AF is pointed out.

Keywords: atrial fibrillation, RR interval distribution, exponential tail, power spectrum, surface ECG, time series analysis

1. Introduction

Atrial fibrillation (AF) is the most common arrhythmia of the heart and leads to an impairment of physical ability and to a reduction of quality of life (for a review, see e.g. [1]). Connected with these degradations is an increased risk of thromboembolic complications, of strokes [2] and of mortality [3]. The prevalence of AF in the industrialised countries currently is about 1% with respect to the total population and gives rise to tremendous costs for diagnosis and therapy. The risk to develop AF increases with age: For persons older than 40 years 2.3% are affected,

for persons older than 60 years 5.9%, and for persons older than 80 years 8% [4]. Because of the rise of life expectancy in the industrialised countries, the number of persons with AF is likely to increase further.

To support the choice between currently employed therapeutical measures, such as pharmaceutical treatment with antiarrhythmica, AV-nodal ablation or modulation, pulmonary vein or isthmus ablation, and cardioversion, it is necessary to develop a good classification of AF. The size of the left atrium is to date the main parameter to support diagnosis and decisions for treatment options [5, 6], although its role in predicting outcome after a cardioversion is discussed controversially [7, 8]. Further classifications are based on the averaging of P waves [9, 10], on the amplitude of the fibrillatory waves in the surface electro-cardiogram (ECG) [11], or on the morphology of the intra-atrial ECG [12]. The number and degree of spatial uniformity of wave fronts was used for a classification into 3 different AF types [13]. In recent studies short cycle lengths of fibrillatory waves were found to correlate with the risk, that paroxysmal AF changes into persistent AF [14, 15] and that arrhythmica fail to induce conversion to the sinus rhythm [16, 17].

All these established methods use information from intra-atrial signals (or atrial contributions in the surface ECG) to classify AF. However, also ventricular beats show characteristic signatures of AF [18, 19, 20], parts of them have been suggested for the detection of AF [18, 22]. In this work we will show that the distribution of RR intervals during AF exhibits a characteristic exponential tail with a decay rate γ in the range 3-12 Hz. We show that this rate can be determined also in the power spectrum. Our analysis suggests to use γ as an additional classification parameter for AF.

2. Characteristic features of atrial fibrillation in RR interval distributions

Our study is based on RR sequences τ_n of 130 AF patients, which typically comprise 10^5 beats (corresponding to 24h ECG recordings [?]). The probability density $p(\tau)$ of RR intervals for one representative patient is shown in Figs. 1a,b. We find that for large τ, the decay of $p(\tau)$ can be well fitted to an exponential,

$$p(\tau) \sim p_\infty \exp(-\gamma\tau)\,, \tag{1}$$

with decay rate γ and amplitude factor p_∞. This behaviour becomes particularly clear in the semi-logarithmic representation in Fig. 1b.

We find that eq. (1) is a generic feature for AF patients. To quantify the significance of (1) we perform a Kolmogorov-Smirnov test [23] for

the RR intervals in the tail of $p(\tau)$. For sufficient statistical meaning, we require the tail region to encompass at least 0.3 s and at least 2% of the RR intervals. We find that 106 of the 130 AF patients (81.5%) pass the Kolmogorov-Smirnov test with a standard significance level of 10%. Even better values are obtained by a more sophisticated procedure for identifying the parameters γ and p_∞ from an optimal fitting region for eq. (1) as described below.

One can expect that eq. (1) is also specific for atrial fibrillation, since (1) it is not known to be a particular feature of healthy persons. To perform a countercheck, we analyse RR sequences of 72 healthy persons, which were taken from the PhysioNet database [24]. The result for one representative person is displayed in Figs. 1c,d. Clearly, no exponential tail can be identified. Only 6 of the 72 healthy persons (8.3%) would be accepted according to the Kolmogorov-Smirnov test as specified above.

The rough method to identify the tail yields approximate γ values in the range 3-12 Hz. However, to determine the parameters p_∞ and γ for each patient more precisely, a "best fitting" interval $[\tau_1, \tau_2]$ is calculated for each patient, in which the Kolmogorov-Smirnov deviation is smallest. In addition to the requirement that the tail region should encompass at least 2% of the total number of RR intervals, we vary both τ_1 and τ_2 under the constraints *(i)* $\tau_2 - \tau_1 \geq 0.3$ s and *(ii)* $\tau_1 > 0.7$ s. The first constraint *(i)* guarantees that, in the case of small γ, the width of the fitting region covers about one decay time $1/\gamma$. In the case of large γ, it ensures that the fitting interval covers several $1/\gamma$ so that it is not influenced by short-time fluctuations. The second constraint *(ii)* in combination with *(i)* ensures that the fitting region lies right to the maximum of $p(\tau)$. In the best fitting region, 125 of the 130 AF patients (96.2%) pass the Kolmogorov-Smirnov test with significance level 10% and these are taken into account in the following analysis. The fitting region has a mean width of 0.42 s and on average comprises 8.6% of the RR intervals. The histogram of γ values for these patients is displayed in Fig. 2. The values lie in the range 2-12 Hz and have a mean 5.4 Hz.

While almost all $p(\tau)$ of the AF patients show the exponential tail, the shapes of the distributions differ outside the tail region. The shapes can be grouped into classes according to the number of local maxima in $p(\tau)$ (unimodal or multimodal distributions). The physiological origin of multimodal distributions is still under investigation and mostly associated with the presence of different conduction pathways through the AV node [25, 26, 27].

A full account for the unimodal distributions can be obtained by assuming that τ results from a superposition of two statistically independent times, $\tau = \tau' + \eta$, where τ' is drawn from a Gaussian distribution $\psi(\tau')$ with mean τ_G and variance σ_G^2, and η is drawn

from an exponential distribution $\phi(\eta) = \gamma \exp(-\gamma\eta)$ [28]. In order for the times τ' to be positive one could formally introduce a truncated Gaussian, but because it turns out that $\psi(\tau')$ is sufficiently sharply peaked at τ_{G}, we can ignore the truncation. Then we obtain

$$
\begin{aligned}
p(\tau) &= \int_{-\infty}^{\tau} d\tau' \, \psi(\tau') \, \phi(\tau - \tau') \\
&= \frac{\gamma \exp(\gamma\tau_{\mathrm{G}} + \gamma^2\sigma_{\mathrm{G}}^2/2)}{2} \, \mathrm{erfc}\left(\frac{\tau_{\mathrm{G}} + \gamma\sigma_{\mathrm{G}}^2 - \tau}{\sqrt{2}\sigma_{\mathrm{G}}} \right) \exp(-\gamma\tau) \quad (2)
\end{aligned}
$$

with mean $\bar{\tau} = \tau_{\mathrm{G}} + \gamma^{-1}$ and variance $\sigma^2 = \sigma_{\mathrm{G}}^2 + \gamma^{-2}$. Hence, given the γ values as determined above, fits to eq. (2) can be easily performed by just calculating $\bar{\tau}$ and σ^2. These fits are in good agreement for all 48 AF patients with a unimodal distribution. For the representative example in Figs. 1a,b. this is demonstrated by the solid lines. For large RR intervals the distribution follows eq. (1) with

$$
p_{\infty} = \gamma \exp\left(\gamma\tau_{\mathrm{G}} + \frac{\gamma^2\sigma_{\mathrm{G}}^2}{2} \right) = \gamma \exp\left(\gamma\bar{\tau} + \frac{\gamma^2\sigma^2}{2} - \frac{3}{2} \right) \qquad (3)
$$

As shown in Fig. 3 the p_{∞} determined by the linear regression follow closely the theoretical curve predicted by eq. (3). This allows us to scale the exponential tails for these AF patients onto a common master curve, see the inset of Fig. 3. The τ_{G} and σ_{G} lie in the ranges $0.3 - 0.85$ s and $0.04 - 0.17$ s respectively.

The decay rate γ can be viewed as a new parameter for a further classification of AF. As such, it may be subjected to diurnal variations as, for example, the fibrillation rate [29]. To test this, we next study correlations between γ and τ_{G}, which can be expected to be larger during night than day time. The sequences of RR intervals are split into segments of 2^{14} intervals (corresponding to typically 4.5 hours). For good temporal resolution, the analysis is performed on overlapping segments shifted by 2^{12} beats (corresponding to typically 1 hour). In each segment i, γ_i is determined from the RR interval distribution belonging to this segment as described above, and $\tau_{\mathrm{G},i} = \bar{\tau}_i - \gamma_i^{-1}$ is calculated from the the mean $\bar{\tau}_i$ in the segment.

Figure 4a shows the results for a representative patient. Clearly, time periods with larger τ_{G} correspond to periods of smaller γ and vice versa. To quantify this behaviour we calculated the cross correlation coefficient C for all AF patients. The histogram of C values in Fig. 4b reflects pronounced anti-correlations. The mean correlation coefficient is $\bar{C} = -0.86$.

3. Relation to properties of the power spectrum

Properties of the power spectrum $S(f)$ of the RR interbeat intervals [30] during AF have been studied previously by some of the authors and coworkers [20, 21]. For low frequencies $S(f)$ exhibits a $1/f$ type behaviour as known also for healthy persons. At higher frequencies, however, striking differences between the power spectra of healthy persons and AF patients are found (see Fig. 5a for a representative example). While the $1/f$ type behaviour continues up to the highest frequencies for the healthy persons, there is a crossover to an extended part with a behaviour close to white noise at high frequencies for the AF patients. The question arises if the two characteristic features, i.e. the exponential tail in the distribution of RR intervals and the white noise part in the power spectrum, are interrelated due to a generic underlying mechanism.

Motivated by the successful decomposition of the RR intervals τ into two contributions τ' and η, we suppose the exponentially distributed times η to be uncorrelated and hence associated with the white noise part in $S(f)$. By contrast the time τ' should reflect a strongly correlated process associated with the $1/f$ part. Accordingly we write $S(f) = S_{\tau'}(f) + S_{\eta}(f)$, where $S_{\tau'}(f) \sim S_0 f^{-\alpha}$ and $S_{\eta}(f) \simeq S_{\infty}$ are the power spectra of the two contributions. Then the crossover frequency is given by $f_{\times} = (S_0/S_{\infty})^{1/\alpha}$. The strength S_{∞} of the white noise should be given by the decay rate γ (since $S_{\infty} = S_{\eta}(f) = S_{\eta}(f \rightarrow 0)$, and the zero-frequency limit of a power spectrum equals the variance),

$$S_{\infty} = 1/\gamma^2 \,. \tag{4}$$

Using (4), we determined $\gamma_{\mathrm{pow}} \equiv S_{\infty}^{-1/2}$ by averaging $S_{\eta}(f)$ over the modes belonging to the 100 largest frequencies [30]. The result is shown in Fig. 5b in comparison with the decay rate γ obtained from $p(\tau)$. A fair agreement is found for all 48 AF patients. Also, γ_{pow} follows closely the diurnal variations of γ. This can be seen by the dashed line and the hatched bars in Figs. 4b and 4c, respectively. Nevertheless, when doing the time-resolved analysis, the γ obtained from the RR interval distribution and the power spectrum are not as close as in Fig. 4b. This is due to the fact that a precise determination of γ from the RR interval distribution becomes rather difficult for a comparatively small number of RR intervals. By contrast, the white noise part in the power spectrum can be clearly identified already for segments comprising 2^{10} beats only. As a consequence, the power spectrum should be preferred for the determination of the new parameter γ in medical applications.

4. Conclusions

In summary we have studied the distribution and correlation properties of heart beat intervals based on long-term (24h) ECG recordings during AF. A characteristic exponential tail in the distribution of heart beat intervals was found, which is absent in healthy controls and can therefore be used as a novel way to characterise AF. We quantify the tail with the decay rate γ and find values in the range 3–12 Hz. Surprisingly, these γ values can also be determined from the white noise part of the power spectrum. The findings can be described by decomposing the RR intervals into two statistically independent times, where the first one belongs to a correlated process with the typical $1/f$ noise characteristics (as found also for healthy subjects), while the second one belongs to an uncorrelated process. The uncorrelated process is responsible for the occurrence of the exponential distribution and the white noise. Over the day the γ values vary slowly and these variations are anticorrelated with the mean interval belonging to the correlated process. While the time-resolved analysis is rather difficult to perform based on the distribution function, it is straightforwardly carried out based on the power spectrum.

It is remarkable that the range of γ values as well as its diurnal variations are comparable to the range and diurnal variations of the fibrillation rates typically found in medical studies [31, 32, 29]. While it is currently unclear if this is a mere accident or if there exists a deeper connection, the potential of the new parameter γ for the clinical diagnosis should be evaluated. This parameter is readily available from the surface ECG and accordingly easier to obtain than data from intra-atrial recordings. Similar to the fibrillation rate, γ may provide a useful measure to estimate the outcome of a cardioversion or of pharmaceutical treatments. Among others, it could also help to predict the risk that patients with paroxysmal AF develop chronical AF. We hope that our findings will stimulate further research in this direction.

Apart from this issue of practical importance, the results require an explanation based on physiological mechanisms connected with AF. For such explanation both the statistics of atrial impulses and the transduction of them through the atrio-ventricular node are expected to play a key role. On may assume that the observed statistics directly reflect statistical features of the intra-atrial beats. However, typical recordings in the right atria show a rather narrow distribution of the intervals between successive atrial impulses and therefore do not support this idea. On the other hand, it has been suggested that blocked atrial impulses can prolongate the (absolute or relative) refractory period of the atrio-ventricular node, and this process could be a possible reason

for the peculiar statistics of the long heart beat intervals during AF. Further studies, however, are needed to clarify this possibility.

References

1. Nattel, S.: New ideas about atrial fibrillation 50 years on., *Nature* **415** (2002), 219-226.
2. Wolf, P.A., Abbott, R.D. and Kannel, W.B.: Atrial fibrillation as an independent risk factor for stroke: the Framingham Study, *Stroke* **22** (1991), 983-988.
3. Benjamin, E.J., Wolf, P.A., D'Agostino, R.B., Silbershatz, H., Kannel, W.B. and Levy D.: Impact of atrial fibrillation on the risk of death: The Framingham Heart Study, *Circulation* **98** (1998), 946-952.
4. Krahn, A.D., Manfreda, J., Tate, R.D., Mathewson, F.A. and Cuddy, T.E.: The natural history of atrial fibrillation: incidence, risk factors, and prognosis in the Manitoba Follow-Up Study, *Am. J. Med.* **98** (1995), 476-484.
5. Hoglund, C. and Rosenhamer, G.: Echocardiographic left atrial dimension as a predictor of maintaining sinus rhythm after conversion of atrial fibrillation, *Acta Med. Scand.* **217** (1985), 411-415.
6. Verhorst, P.M., Kamp, O., Welling, R.C., van Eenige, M.J. and Visser, C.A.: Transesophageal echocardiographic predictors for maintenance of sinus rhythm after electrical cardioversion of atrial fibrillation, *Am. J. Cardiol.* **79** (1997), 1355-1359.
7. Manabe, K., Oki, T., Tabata, T., Yamada, H., Fukuda, K., Abe, M., Iuchi, A., Fukuda, N. and Ito, S.: Transesophageal echocardiographic prediction of initially successful electrical cardioversion of isolated atrial fibrillation. Effects of left atrial appendage function, *Jpn. Heart J.* **38** (1997), 487-495.
8. Holm, M., Pherson, St., Ingemansson, M., Sörnmo, L., Johansson, R., Sandhall, L., Sunemark, M., Smideberg, B., Olson and Ch., Olsson, S.B.: Non-invasive assessment of the atrial cycle length during atrial fibrillation in man: introducing, validating and illustrating a new ECG method, *Cardiovasc. Res.* **38** (1998), 69-81.
9. Yamada, T., Fukunami, M., Shimonagata, T., Kumagai, K., Sanada, S., Ogita, H., Asano, Y., Hori, M. and Hoki, N.: Dispersion of signal-averaged P wave duration on precordial body surface in patients with paroxysmal atrial fibrillation, *Eur. Heart J.* **20** (1999), 211-220.
10. Raitt, M.H., Ingram, K.D. and Thurman, S.M.: Signal-averaged P wave duration predicts early recurrence of atrial fibrillation after cardioversion, *Pacing Clin. Electrophysiol.* **23** (2000), 259-265.
11. Peter, R.H., Morris Jr., J.J. and McIntosh, H.D.: Relationship of fibrillatory waves and P waves in the electrocardiogram, *Circulation* **33** (1966), 599-606.
12. Wells Jr., J.L. Karp, R.B., Kouchoukos, N.T., MacLean, W.A., James, T.N. and Waldo, A.L.: Characterization of atrial fibrillation in man: studies following open heart surgery, *Pacing Clin. Electrophysiol.* **1** (1978), 426-38.
13. Konings, K.T., Kirchhof, C.J., Smeets, J.R., Wellens, H.J., Penn, O.C. and Allessie, M.A.: High-density mapping of electrically induced atrial fibrillation in humans, *Circulation* **89** (1994), 1665-80.

14. Asano, Y., Saito J., Matsumoto K., Kaneko K., Yamamoto, T. and Uchida, M.: On the mechanism of termination and perpetuation of atrial fibrillation, *Am. J. Cardiol.* **69** (1992), 1033-1038.

15. Boahene, K.A., Klein, G.J., Yee, R., Sharma, A.D. and Fujimura, O.: Termination of acute atrial fibrillation in the Wolff-Parkinson-White syndrome by procainamide and propafenone: importance of atrial fibrillatory cycle length, *J. Am. Coll Cardiol.* **16** (1990), 1408-1414.

16. Stambler, B.S., Wood, M.A. and Ellenbogen K.A.: Antiarrhythmic actions of intravenous ibutilide compared with procainamide during human atrial flutter and fibrillation: electrophysiological determinants of enhanced conversion efficacy, *Circulation* **96** (1997), 4298-4306.

17. Bollmann, A., Binias, K.-H., Toepffer, I., Molling, J., Geller, Ch. and Klein, H.U.: Importance of left atrial diameter and atrial fibrillatory frequency for conversion of persistent atrial fibrillation with oral flecainide, *Am. J. Card.* **90** (2002), 1011-1014.

18. Moody, G. and Mark, R. A new method for detecting atrial fibrillation using RR-intervals, *Comp. Card.* **10** (1983), 227-230.

19. Pinciroli, F. and Castelli, A.: Pre-clinical experimentation of a quantitive synthesis of the local variability in the original R-R interval sequence in the presence of arrhytmia, *Automedica* **6** (1986), 295-317.

20. Hayano, J., Yamasaki, F., Sakata, S., Okada, A., Mukai, S. and Fujinami, T.: Spectral characteristics of ventricular response to atrial fibrillation, *Am. J. Physiol.* **273** (1997), H2811-H2816.

21. Heinrichs, S., Struzik, Z.R., Hayano, J. and Yamamoto, Y.: Probing temporal correlation in ventricular interbeat intervals during atrial fibrillation with local continuous DFA, *Proceedings of SPIE Second International Symposium on Fluctuations and Noise*, Vol. **5467** (2004), 404-410.

22. Pinciroli, F., Rossi,, R. and Valenca, P.: PAFHPI: self-monitoring of paroxysmal atrial fibrillation episodes in ambulatory patients. In: Proceedings Computers in Cardiology, (London, IEEE Computer Society Press, 1993), p. 503-506.

23. Honerkamp, J.: Stochastic Dynamical Systems (VCH Publishers, Cambridge, 1994), ch. 3.2.5.

24. Datsets of 54 persons were obtained from the "Normal Sinus Rhythm Database" and of 18 persons from the "Normal Sinus Rhythm RR Interval Database" (see http://www.physionet.org/).

25. Rokas, St., Gaitanidou, St., Chatzidou, S., Pamboucas, C., Achtipis, D. and Stamatelopoulos, St.: Atrioventricular Node Modification in Patients With Chronic Atrial Fibrillation - Role of Morphology of RR Interval Variation, *Circulation* **103** (2001), 2942-2948.

26. Hatzido, S. N., Gaitanidou, Ch., Paboukas, K. A., Vogiatzis, St. D., Antonellis, I. and Rokas, St. G.: Modification of the Atrioventricular Node in Patients with Chronic Atrial Fibrillation. - The Role of RR Interval Distribution Pattern, *Hellenic. J. Cardiol.* **43** (2002), 116-126.

27. Weismuller, P., Kratz, C., Brandts, B., Kattenbeck, K., Trappe, HJ. and Ranke, C.: AV nodal pathways in the R-R interval histogram of the 24-hour monitoring ECG in patients with atrial fibrillation, *Ann. Noninvasive Electrocardiol.* **6** (2001), 285-9.

28. For multimodal distributions one can adopt an analogous procedure but should take into account that τ' is drawn from a convolution of several Gaussians.

29. Meurling, C. J., Waktare, J. E. P., Holmqvist, I., Hedman, A., Camm, A. J., Olsson, S. B. and Malik, M.: Diurnal variations of the dominant cycle length of chronic atrial fibrillation, *Am. J. Physiol. Heart Circ. Physiol.* **280** (2001), H401-H406.

30. The power spectrum of the sequence of RR interbeat intervals τ_n, $n = 0, \ldots, N - 1$ is calculated by $S(f_m) = |\hat{\tau}(f_m)|^2/N$ for $f_m = m/N$, $m = -N/2, \ldots, N/2 - 1$, where $\hat{\tau}(f_m) = \sum_{n=0}^{N-1} (\tau_n - \bar{\tau}) \exp(-2\pi i f_m n)$.

31. Gaita, F., Riccardi, R., Calo, L., Scaglione, M., Garberoglio, L., Antolini, R., Kirchner, M., Lamberti, F., and Richiardi, E.: Atrial mapping and radiofrequency catheter ablation in patients with idiopathic atrial fibrillation. Electrophysiological findings and ablation results, *Circulation* **97** (1998), 2136-45.

32. Hobbs, W. J., Fynn, S., Todd, D. M., Wolfson, P., Galloway, M., Garratt, C. J., Reversal of atrial electrical remodeling after cardioversion of persistent atrial fibrillation in humans, *Circulation* **101** (2000), 1145-51.
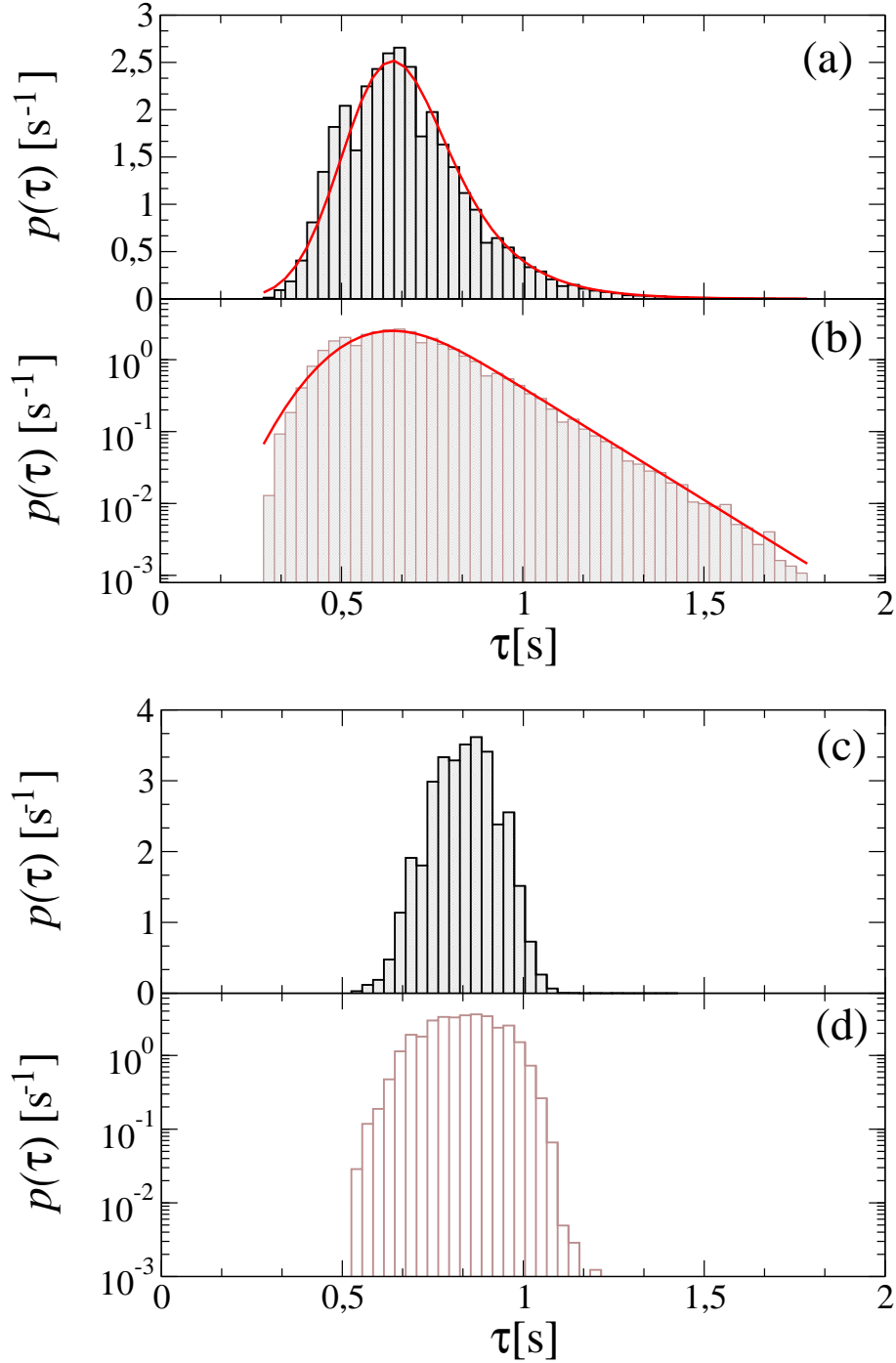
Figure 1. Probability density $p(\tau)$ of RR intervals τ for one representative AF patient on *(a)* linear and *(b)* semi-logarithmic scale. In the calculation a fixed bin width of 0.03 s was used. The lines mark the fit to eq. (2) with the exponential decay for large τ (cf. eq. (1)). Corresponding plots on *(c)* linear and *(d)* semi-logarithmic scale of one representative healthy person show no signature of an exponential decay.
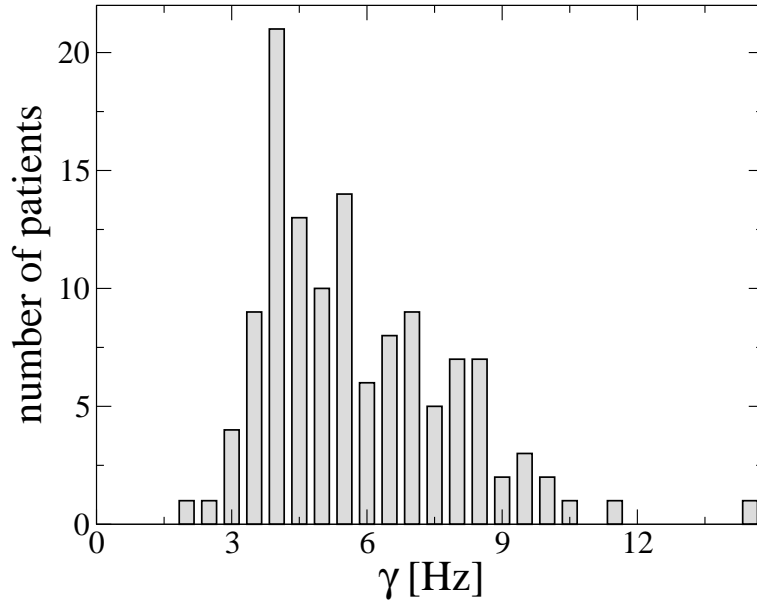
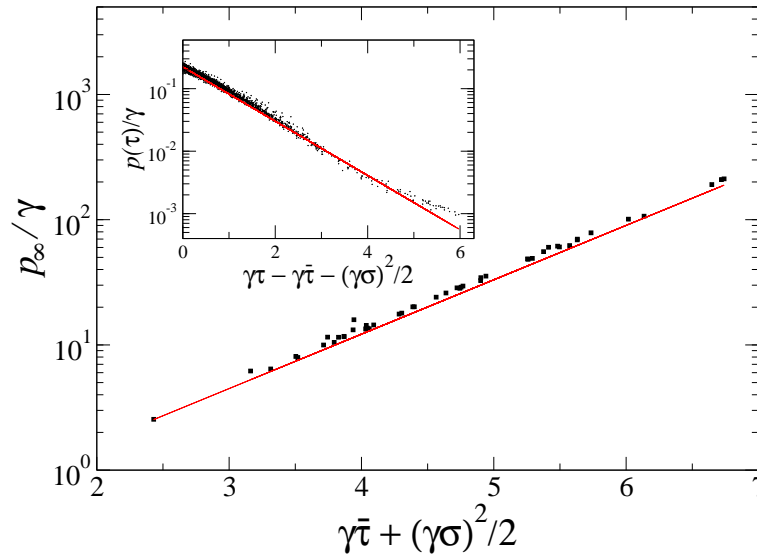*Figure 2.* Histogram of γ values with mean 5.4 Hz and standard deviation 2.1 Hz for all 125 patients.

Figure 3. Semi-logarithmic plot of p_∞/γ for the subgroup of 48 patients as a function of $\gamma\bar{\tau}+\gamma^2\sigma^2/2$. The straight line marks the theoretical behaviour according to eq. (3). The inset shows the rescaled probability density for this group of patients.
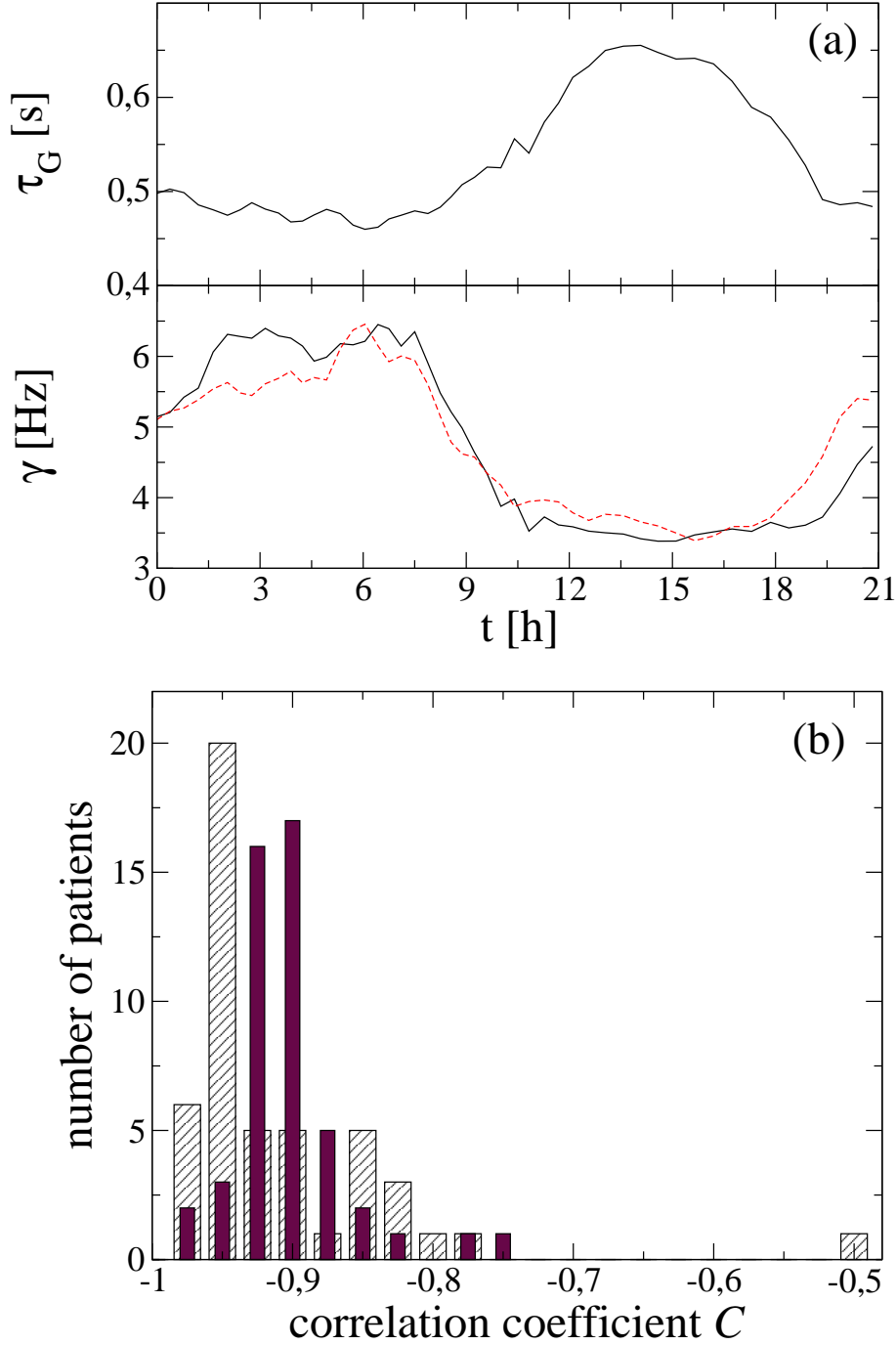
Figure 4. (a) Time dependence of τ_G and decay rate γ in segments of 2^{14} beats during AF (solid line: γ calculated from the RR interval distribution; dashed line: $\gamma = \gamma_\mathrm{pow}$ calculated from the power spectrum, see Sec. 3). The segments were shifted by 2^{12} beats, and $\tau_{\mathrm{G},i}$ and γ_i are assigned to the starting point of each segment i. (b) Histogram of cross-correlation coefficients $C = \sum_{i=1}^{N}(\tau_{\mathrm{G},i} - \tilde{\tau})(\gamma_i - \tilde{\gamma})/(N\Delta_\gamma \Delta_\tau)$, where N is the number of segments, $\tilde{\tau} = \sum_{i=1}^{N}\tau_{\mathrm{G},i}/N$, $\tilde{\gamma} = \sum_{i=1}^{N}\gamma_i/N$, and Δ_τ, Δ_γ are the corresponding standard deviations (full bars: γ_i calculated from the RR interval distribution; hatched bars: γ_i calculated from the power spectrum, see Sec. 3).
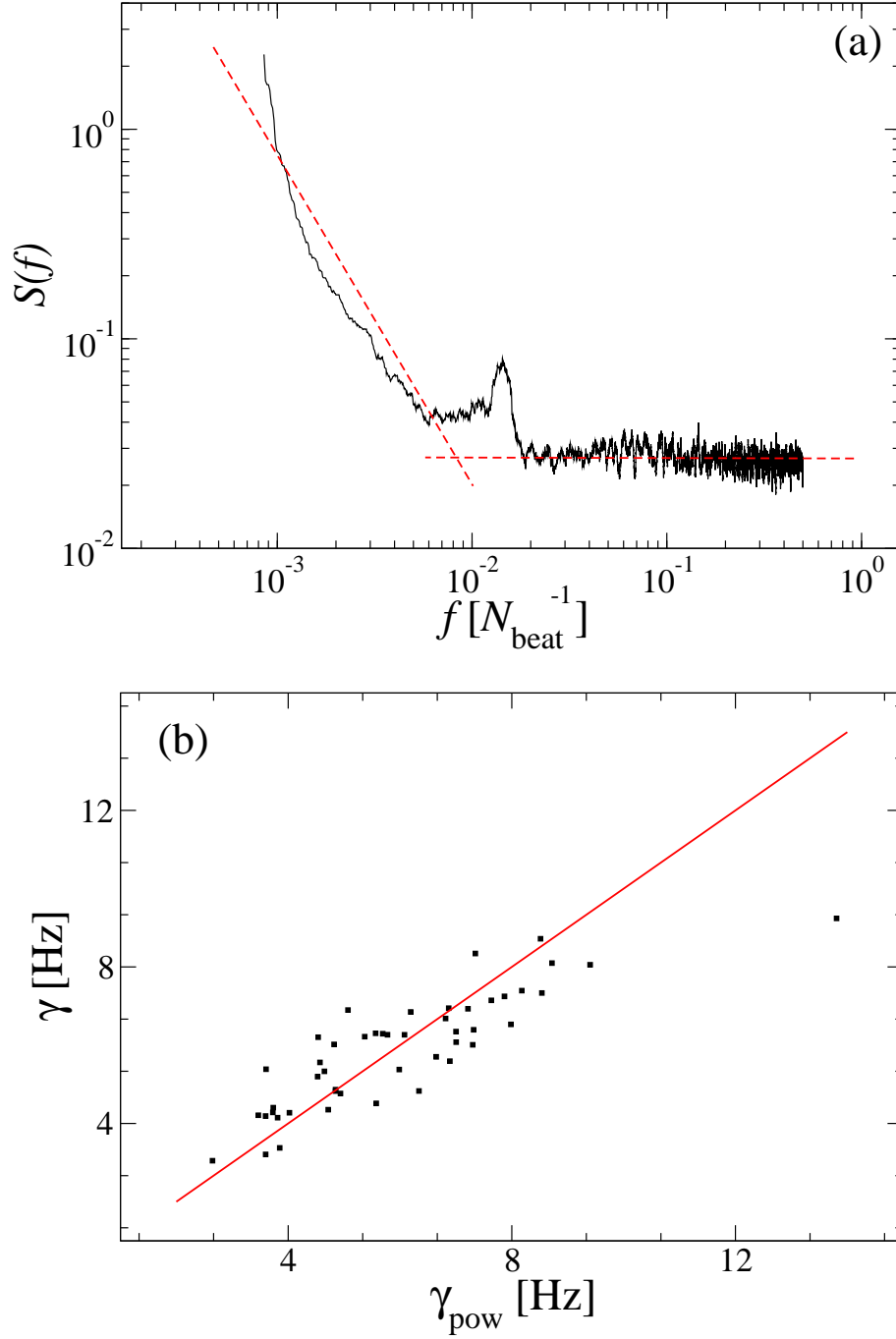
Figure 5. (a) Power spectrum of RR intervals τ for one representative AF patient on a double-logarithmic scale. The spectrum exhibits a distinct crossover at a frequency $f_{\mathrm{crit}} \simeq (100 \text{ beats})^{-1}$. For frequencies $f < f_{\mathrm{crit}}$ the spectrums exhibit the typical $1/f$ behaviour and a white noise characteristic for $f > f_{\mathrm{crit}}$. (b) γ vs. γ_{pow} for the group of 48 patients with unimodal $p(\tau)$. The red line marks the theoretical relation $\gamma = \gamma_{\mathrm{pow}}$.